ORNL/CP-95414

CONF-971201--

To be submitted to the Fall ~~1998~~ 1997 MRS Meeting

Ion Beam Synthesis of CdS, ZnS, and PbS Compound Semiconductor Nanocrystals

C. W. WHITE, J. D. BUDAI, A. L. MELDRUM, S. P. WITHROW,
R. A. ZUHR, E. SONDER, A PUREZKY, D. B. GEOHEGAN
Oak Ridge National Laboratory, Oak Ridge, TN

J. G. ZHU
New Mexico State University, Las Cruces, NM

D. O. HENDERSON
Fisk University, Nashville, TN

Prepared by the
Oak Ridge National Laboratory
Oak Ridge, Tennessee 37831
managed by
LOCKHEED MARTIN ENERGY RESEARCH CORP.
for the
U.S. DEPARTMENT OF ENERGY
under contract DE-AC05-96OR22464

December 1997

DISCLAIMER

ION BEAM SYNTHESIS of CdS, ZnS, and PbS COMPOUND SEMICONDUCTOR NANOCRYSTALS

C. W. WHITE,* J. D. BUDAI,* A. L. MELDRUM,* S. P. WITHROW,* R. A. ZUHR,*
E. SONDER,* A. PUREZKY,* D. B. GEOHEGAN,* J. G. ZHU,** and
D. O. HENDERSON***
*Oak Ridge National Laboratory, Oak Ridge, TN
**New Mexico State University, Las Cruces, NM
***Fisk University, Nashville, TN

ABSTRACT

Sequential ion implantation followed by thermal annealing has been used to form encapsulated CdS, ZnS, and PbS nanocrystals in SiO_2 and Al_2O_3 matrices. In SiO_2, nanoparticles are nearly spherical and randomly oriented, and ZnS and PbS nanocrystals exhibit a bimodal size distribution. In Al_2O_3, nanoparticles are facetted and coherent with the matrix. Initial photoluminescence (PL) results are presented.

INTRODUCTION

The unusual properties of compound semiconductor nanocrystals compared to bulk materials has stimulated considerable interest in exploring new methods to fabricate these materials [1-3]. Ion implantation is a very versatile technique which has been used recently to form a wide range of elemental and compound semiconductor nanocrystals encapsulated in a variety of host materials [4-5]. In this method, individual constituents of the desired compound are implanted sequentially at energies chosen to give an overlap of the profiles. If the individual constituents are insoluble in the matrix, then thermal annealing (or implantation at elevated temperatures) leads to precipitation, and the compound forms if the constituents have a strong chemical affinity for each other. In this paper, we demonstrate that this method can be used to form CdS, ZnS, and PbS nanocrystals encapsulated in matrices of SiO_2 and Al_2O_3. Nanocrystals of CdS have been fabricated previously by chemical methods in colloidal solution [6], by arrested precipitation [7], or encapsulated in glass through heat treatment of doped glasses [8,9] and their size-dependent optical properties have been investigated. ZnS nanoparticles have been prepared previously in colloidal solution [6] or powder form and when doped with impurities (Mn, Cu) have attracted interest recently as high-quantum efficiency luminescent materials [10-11]. PbS nanocrystals have been proposed as photocatalysts for energy applications and have been synthesized in inverse micells [12].

EXPERIMENTAL

Substrates used in this work were fused silica (SiO_2), thermally oxidized silicon (SiO_2/Si), or c-axis oriented Al_2O_3 single crystals. To form compound semiconductor nanocrystals in these substrates, the individual constituents were implanted sequentially at energies chosen to give an overlap of the profiles. Implants were carried out at room temperature in SiO_2 and at 550° in Al_2O_3 in order to keep the matrix crystalline during implantation. Stochiometry is determined by the implanted dose. Both Gaussian profiles resulting from single energy implants as well as flat profiles resulting from multiple energy implants have been used. Following implantation, samples were annealed for 1 h in flowing Ar + 4% H_2 to induce precipitation and nanocrystal formation. Samples were characterized using a variety of techniques including Rutherford backscattering, X-ray diffraction (Cu-Kα), and transmission electron microscopy (TEM). PL spectra were obtained from selected samples using 457 nm or 248 nm excitation.

RESULTS

X-ray diffraction results demonstrating the formation of CdS nanocrystals in SiO_2 and Al_2O_3 are shown in Figs. 1 and 2. In SiO_2 (Fig. 1), diffuse scattering from SiO_2 is observed in addition

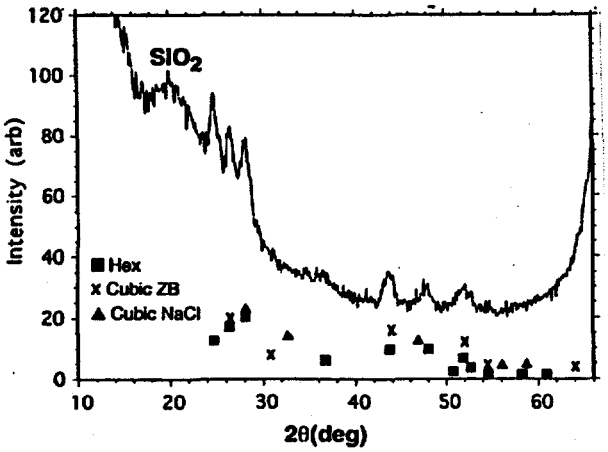

Fig. 1. X-ray diffraction results showing the formation of CdS nanocrystals in SiO_2/Si. Equal concentrations (5.3×10^{21}/cm^3) of Cd and S were implanted to a depth of ~180 nm.

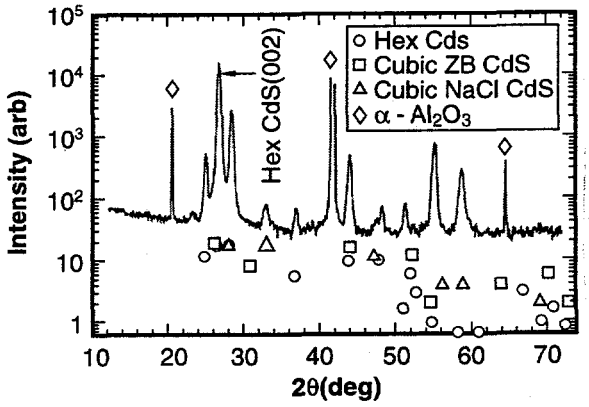

Fig. 2. X-ray diffraction from CdS nanocrystals in Al_2O_3. Equal doses (4.3×10^{16}/cm^2) of Cd (450 keV) and S (0.164 keV) were implanted at 550°C.

to strong lines arising from CdS. In Al_2O_3, there are a multitude of diffraction lines arising fromCdS, in addition to the expected diffraction from the matrix. The position and relative intensity of X-ray lines characteristic of the hexagonal CdS and the two possible cubic structures (ZB and NaCl) are indicated in Figs. 1 and 2 (from powder files). Detailed analysis of the X-ray diffraction results show that most of the CdS nanocrystals in both SiO_2 and Al_2O_3 have the hexagonal structure. In addition, the CdS nanocrystals in Al_2O_3 are coherent with the matrix having their (002) planes parallel to the c-planes of Al_2O_3. These nanoparticles exhibit strong in-plane alignment also. Therefore, oriented CdS nanoparticles with hexagonal structure are produced in Al_2O_3 if implantation is carried out at elevated temperatures. By contrast, we find that the cubic structure is produced if implantation is done at low temperature where we form the amorphous phase during implantation [13].

Figures 3 and 4 are X-ray diffraction results demonstrating the formation of ZnS (Fig. 3) and PbS (Fig. 4) in SiO_2 and Al_2O_3 as a result of implantation and annealing. ZnS has hexagonal and cubic structures, and the ZnS nanocrystals produced in SiO_2 and Al_2O_3 by ion implantation are a mixture of the two structures. In SiO_2, the nanocrystals are randomly oriented, but in Al_2O_3, they are coherent with the lattice and are oriented predominantly with the (002) planes of the hexagonal ZnS and the (111) planes of cubic ZnS parallel to the c-planes of Al_2O_3. In Al_2O_3, the ZnSnanoparticles also exhibit strong in-plane orientation.

Figure 4 shows that cubic PbS nanocrystals are formed in both SiO_2 and Al_2O_3 as a result of ion implantation and annealing. In SiO_2, the nanoparticles are randomly oriented, but in Al_2O_3, they are coherent with the lattice and are oriented predominantly with their (002) planes parallel to the c planes of Al_2O_3.

Figures 5 and 6 are cross-section TEM micrographs showing the microstructures in the near-surface region of SiO_2 and Al_2O_3 samples containing CdS, ZnS, and PbS nanocrystals. In Fig. 5, CdS nanocrystals are nearly spherical and have an average diameter that is slightly larger than 100 Å. Nanocrystals of smaller size are formed when the Cd + S concentration is reduced. By contrast, ZnS and PbS nanocrystals exhibit a pronounced bimodal size distribution with a few large nanocrystals (several hundred angstroms diameter) in addition to a large number of smaller nanocrystals. The large nanocrystals form in well-defined spatial regions, being predominantly located in the vicinity of the end-of-range in the case of ZnS, and near the peak of the implanted profile for the case of PbS. These larger particles presumably develop as a result of diffusion controlled Ostwald ripening, but why they form in such localized regions is not understood and is currently under investigation.

High-resolution micrographs showing CdS, ZnS, and PbS nanoparticles in Al_2O_3 are shown in Fig. 6. In contrast to the case of SiO_2 where nanocrystals are nearly spherical, in Al_2O_3 the nanocrystals exhibit pronounced faceting. The average size of these nanoparticles is also greater than in the case of SiO_2.

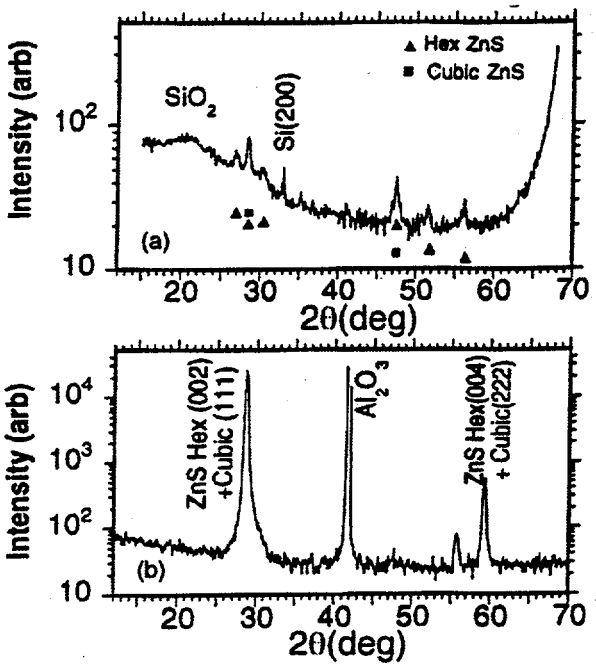

Fig. 3. X-ray diffraction from ZnS nanocrystals formed in SiO_2/Si (a) and Al_2O_3 (b). In (a) equal concentrations (7.5×10^{21}/cm^3) of Zn and S were implanted to a depth of 250 nm. In (b) equal doses (6×10^{16}/cm^2) of Zn (280 keV) and S (150 keV) were implanted at 400°C.

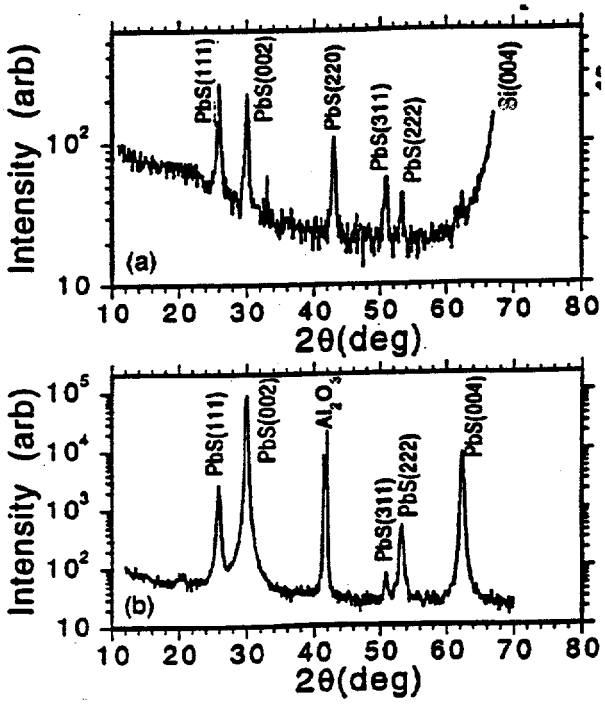

Fig. 4. X-ray diffraction from PbS nanocrystals formed in SiO_2/Si (a) and Al_2O_3 (b). In (a) equal doses (5×10^{16}/cm^2) of Pb (320 keV) and S (82 keV) were implanted. In (b) equal doses (5×10^{16}/cm^2) of Pb (850 keV) and S (180 keV) were implanted at 550°C.

These nanoparticles give rise to strong optical absorption and in some cases strong photoluminescence. In this paper, we show some of the PL results. Figure 7 shows PL arising from CdS nanocrystals in SiO_2. After annealing (1000°/1 h), the peak in the PL spectra at 510 nm is very close to the bandgap of CdS (2.43 eV) and we attribute this peak to recombination of excitons in the nanocrystals. There is also a broad PL band at lower energies which probably arises from surface-related defects, as others [9] have discussed.

Figure 8 shows the PL spectra arising from CdS nanocrystals in Al_2O_3. In the as-implanted state there is little or no PL, but after annealing, there is intense bandedge PL arising from recombination of excitons in the CdS nanoparticles. PL from the nanoparticles is blue shifted relative to that of a standard, and this may be the result of quantum confinement, but more likely results from lattice strain. In Al_2O_3, there is little or no PL at lower energies and this suggests that surface defects are relatively less important than when these particles are encapsulated in SiO_2 (see Fig. 7).

ZnS nanoparticles also give rise to strong PL as demonstrated in Fig. 9. In this case, the PL occurs at energies less than the bandgap, and this suggests that defects or surface states are responsible for the emission. The spectra is similar to that reported in ref. 12 for ZnS nanoparticles synthesized by chemical means and attributed to a deficiency of S in the nanoparticles.

CONCLUSIONS

Sequential ion implantation and thermal annealing has been used to form CdS, ZnS, and PbS nanoparticles in SiO_2 and Al_2O_3. In SiO_2, the nanoparticles are nearly spherical and randomly oriented. Bimodal size distributions are observed for ZnS and PbS in SiO_2. In Al_2O_3, nanoparticles are coherent with the lattice and when implantation is carried out at elevated temperature, CdS has the hexagonal structure. ZnS is a mixture of hexagonal and cubic structures and PbS has the cubic structure in both Al_2O_3 and SiO_2. Strong PL is observed from CdS

nanoparticles in both SiO_2 and Al_2O_3. ZnS nanoparticles in SiO_2 show strong PL but at energies smaller than the bandgap.

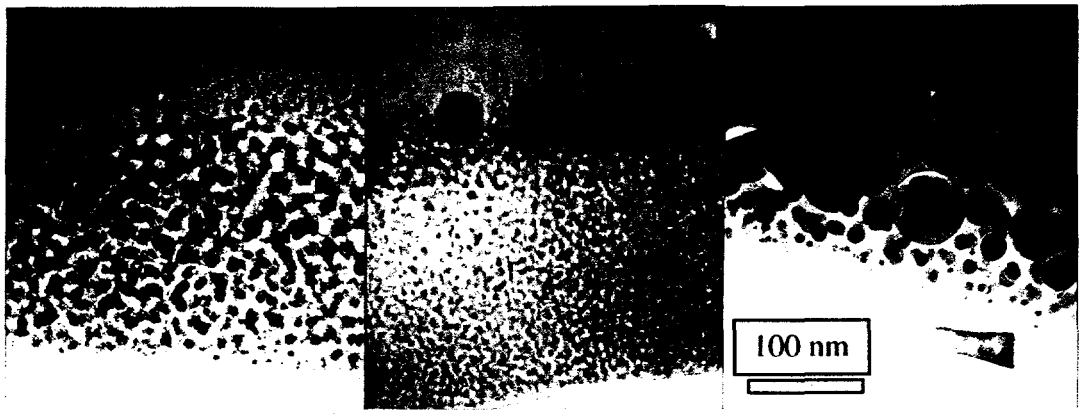

Fig. 5. Cross-section micrographs showing CdS (left), ZnS (center), and PbS (right) nanocrystals in SiO_2. Implantation and annealing condiitions are given in the captions of Fig. 1 (CdS), Fig. 3a (ZnS), and Fig. 4a (PbS).

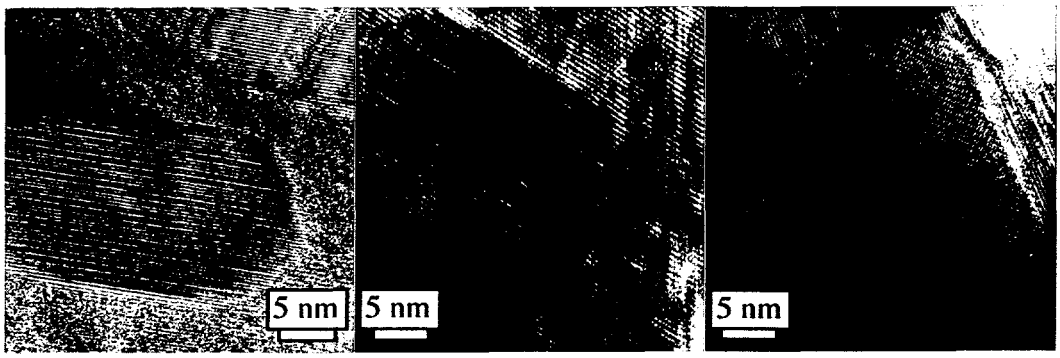

Fig. 6. High-resolution cross-section micrographs showing ZnS (left), PbS (center), and CdS (right) nanocrystals in Al_2O_3. Implantation and annealing conditions are given in the captions of Fig. 2 (CdS), Fig. 3b (ZnS), and Fig. 4b (PbS).

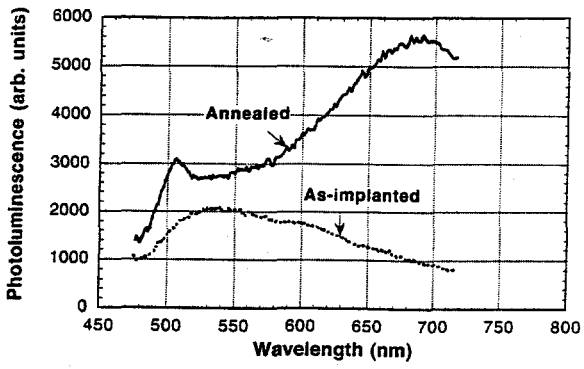

Fig. 7. PL spectra (excited at 457 nm) arising from encapsulated CdS nanocrystals in SiO_2 formed by the implantation of equal doses ($1 \times 10^{17}/cm^2$) of Cd (450 keV) and S (164 keV).

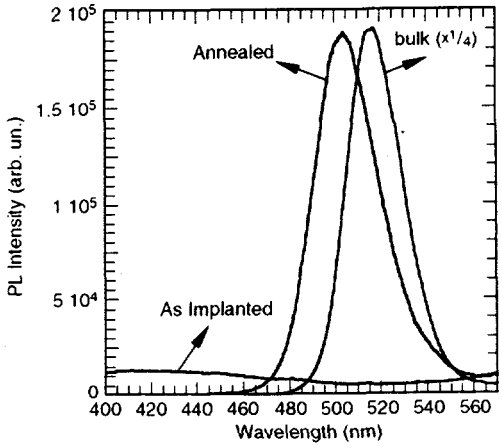

Fig. 8. PL spectra (excited at 248 nm) from CdS nanocrystals in Al_2O_3. Implant conditions are the same as those in Fig. 2. PL spectra from bulk CdS is shown for comparison.

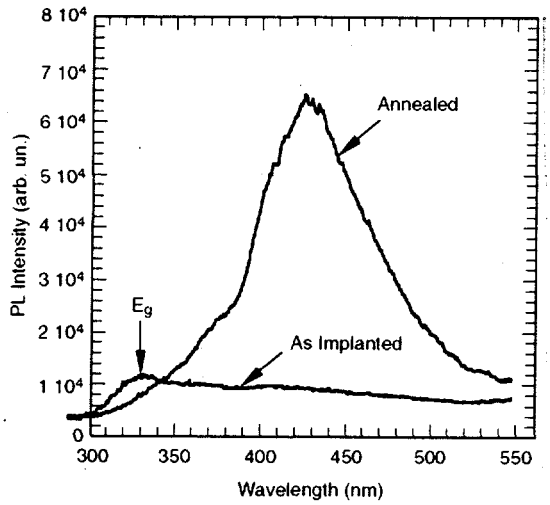

Fig. 9. PL spectra (excited at 248 nm) from ZnS nanocrystals in SiO_2. Equal concentrations ($1.5 \times 10^{21}/cm^3$) of each constituent were implanted to a depth of ~250 nm prior to annealing. E_g denotes the energy of the bulk bandgap.

Oak Ridge National Laboratory, managed by Lockheed Martin Energy Research Corp. for the U.S. Department of Energy under contract number DE-AC05-96OR22464.

REFERENCES

1. "Microcrystalline and Nanocrystalline Semiconductors," ed. by L. Brus, R. W. Collins, M. Hiroshi, F. Koch, and C. C. Tsai, Mat. Res. Soc. Proc. **358** (MRS, Pittsburgh, 1995).

2. "Advances in Microcrystalline and Nanocrystalline Semiconductors–1996," ed. by A. P. Alivisatos, P. Fauchet, I. Shimizu, R. Collins, T. Shimuder, and J. C. Vial, Mat. Res. Soc. Proc. **452** (MRS, Pittsburgh, 1997).

3. A. P. Alivisatos, Science **271**, 933 (1996).

4. C. W. White, J. D. Budai, S. P. Withrow, J. G. Zhu, S. J. Pennycook, R. A. Zuhr, D. M. Hembree, Jr., D. O. Henderson, R. H. Magruder, M. J. Yacaman, G. Mondragon, and S. Prawer, Nucl. Instrum. Methods in Physics Res. B **127/128**, 545 (1997).

5. J. D. Budai, C. W. White, S. P. Withrow, R. A. Zuhr, and J. G. Zhu, Mat. Res. Soc. Proc. **452**, 89 (1997).

6. R. Rossetti, R. Hull, J. M. Gibson, and L. E. Brus, J. Chem. Phys. **82**, 552 (1985).

7. C. B. Murray, D. J. Norris, and M. G. Bawendi, J. Am. Chem. Soc. **115**, 8706 (1993).

8. V. Sukumar and R. H. Doremus, Phys. Stat. Sol. (b) **179**, 307 (1993).

9. B. G. Potter and J. H. Simmons, Phys. Rev. B **37**, 10838 (1988).

10. R. N. Bhargava, D. Gallagher, X. Hong, and A. Nurmikko, Phys. Rev. Lett. **72**, 416 (1994).

11. A. Khosravi, M. Kundu, L. Jatwa, S. K. Deshpande, U. A. Bhagwat, M. Sastry, and S. K. Kulkarni, Appl. Phys. Lett. **67**, 2702 (1995).

12. D. E. Bliss, J. P. Wilcoxon, P. P. Newcomer, and G. A. Samara, Mat. Res. Soc. Proc. **358**, 265 (1995).

13. J. D. Budai, C. W. White, S. P. Withrow, M. F. Chisholm, J. G. Zhu, and R. A. Zuhr, Nature (in press).